



Contents lists available at SciVerse ScienceDirect

Flow Measurement and Instrumentation

journal homepage: www.elsevier.com/locate/flowmeasinst

Optical tomography hardware development for solid gas measurement using mixed projection

S.Z.M. Muji^b, C.L. Goh^a, N.M.N. Ayob^a, R.A. Rahim^{a,*}, M.H.F. Rahiman^c, H.A. Rahim^a, M.J. Pusppanathan^a, N.S.M. Fadzil^a^a Protom-1, Faculty of Electrical Engineering, University Teknologi Malaysia, 81310 Johor, Malaysia^b Faculty of Electrical and Electronic Engineering, Universiti Tun Hussein Onn Malaysia, 86400 Parit Raja, Johor, Malaysia^c Tomography Imaging Research Group, School of Mechatronic Engineering, Universiti Malaysia Perlis, Pauh Putra Campus, 02600 Arau, Perlis, Malaysia

ARTICLE INFO

Article history:

Received 3 August 2012

Received in revised form

9 May 2013

Accepted 21 May 2013

Available online 6 June 2013

Keywords:

Solid gas measurement

Optical tomography

Mixed projection

ABSTRACT

The ability to implement fan beam projection in parallel view in an optical tomography setup is one of the novelties of this research. This design involves a sensor jig specifically designed for parallel applications that does not involve a collimator. Therefore, the fan beam projections can also be implemented in the same sensor jig without difficulty. This method is a very practical solution for overcoming the disadvantages of parallel beam projection. Although the fan beam has its own disadvantages, combining the fan beam approach with the parallel beam approach is expected to further enhance the optical tomography image quality. The image quality can be measured using the Peak Signal-to-Noise Ratio (PSNR) and the Normalized Mean-Square Error (NMSE) parameters. The combination of the two approaches also eliminates the unwanted noise that appears when using parallel beam projection alone.

© 2013 Elsevier Ltd. All rights reserved.

1. Introduction

The word tomography, meaning a slice of an image, is derived from the Greek word *tomos* ("part" or "section"). Technically, tomography is about obtaining cross-sectional two- or three-dimensional images of *N*-dimensional objects [1]. Tomography has been adopted in many areas of the physical sciences and engineering to measure the distributions ("images") of parameters of interest in various processes [2]. Currently, tomography is practiced in numerous applications in both the medical and industrial fields; the industrial terminology for tomography is process tomography.

It all began in the mid-1980s, when process tomography began to be used in an imaging system [3]. The use of tomography is beneficial in industrial applications that involve multiphase flow, i.e., fluid–fluid flow, fluid gas flow, water oil flow and solid gas flow. Process tomography enables the measurement of many types of parameters, such as the velocity of the material, the concentration profile, the mass flow rate and the particle size. All these parameters can be used in optimizing the design of the process flow. Through tomography techniques, flow can be continuously

monitored without interruption of the flow inside the pipeline, which improves the inspection process in industry. Many industries still perform common methods of monitoring pipeline flow, for example, in the palm oil industry, where the palm oil is separated into useful oil content and wasted sludge content. The sludge content will undergo oil processing procedures again in the pipeline to identify any remaining palm oil [4]. By applying tomography, we can identify the percentage of useful oil and sludge waste in the pipeline. With this knowledge of the fraction of useful oil in the pipeline, we can reduce the processing time and any unnecessary oil refinery processes.

In the solid gas industry, there is a need to monitor and determine the blockages in the pipeline and to verify whether the subjects of the measurement are flowing as required [5]. Moreover, the current systems used in the industry can only provide measurement readings and are unable to identify the material's distribution and movement [6] in the pipeline. Tomography has the ability to visualize the structures inside the pipeline. Therefore, problems such as blockages or unexpected processing results, which may affect or change the flow of the solids and reduce effectiveness, can be easily solved with the help of a tomography system.

A tomography system is setup by mounting a number of sensors along the outer layer of the pipeline to monitor the inner flow and detect any changes in the pipeline. The advantage of the designed system is that it will reduce the cost of operation and

* Corresponding author. Tel.: +60 197104000; fax: +60 75566177.

E-mail addresses: szarina@uthm.edu.my (S.Z.M. Muji), ruzairi@fke.utm.my (R.A. Rahim), hafiz@unimap.edu.my (M.H.F. Rahiman).

may help the company increase its profit and reduce losses. More active research relating to process tomography should be conducted in a more practical way to ensure that the product can be commercialized to fulfill industrial needs. There are areas that can be further improved in this field, as there are still many weaknesses and disadvantages in the current system.

In addition, image ambiguity is another major problem that should be addressed in optical tomography [7]. Image quality can be analyzed using certain parameters, such as the Peak Signal-to-Noise Ratio (PSNR) and the Normalized Mean-Square Error (NMSE). An image with a high PSNR and a low NMSE exhibits an excellent image quality. LBP is the main algorithm used in this project. By using a single type of projection, i.e., the parallel beam projection, the image quality will be quite poor. Therefore, to solve this poor image quality problem, we implemented some modifications that involved combining parallel beam projection with fan beam projection.

2. Optical tomography

The general implementation of optical tomography involves the use of a set of light sources and photo detectors to obtain parallel views of the pipeline. In the optical setup, a beam of light is projected through some medium from one boundary point, and this light beam is detected at another boundary point. At the receiving point, the voltage response of a photo-detector is measured, and any reduction in the response is proportional to the presence of an object in the pipe or vessel, i.e., optical tomography detects the attenuation of the signal caused by the objects to be imaged.

The advantages of optical tomography are:

- (a) negligible response time,
- (b) very high resolution (limited by the wavelength of light),
- (c) reduced effects of electrical noise or interference,
- (d) a wide selection of readily available emitters and detectors, and
- (e) improved spatial resolution over conventional tomography.

Although optical tomography can be regarded as the simplest type of tomography, it also has its drawbacks. Light can travel through non-opaque objects, therefore non-opaque objects cannot be used, as no response will be observed at the receiving end.

In addition, an opaque object is the most suitable material to be measured, but problems occur when two objects overlap each other, as it is difficult to distinguish them. This overlapping issue can be solved by using many projections and also by combining the parallel and fan beam approaches. This solution is the approach taken in the research described in this paper.

2.1. Recent research in optical tomography

There are many research groups that have established their own niche in optical tomography. Sheffield Hallam University, for example, focuses on a variety of experiments which utilize optical sensors [8–10]. Ongoing research at the Universiti Teknologi Malaysia (UTM) focuses on solid gas, where both parallel and fan beam projection is being used. Infrared LEDs, lasers and fiber optics are typically used in their research [11–17]. Another related group from Zhejiang University, China, focused on near-infrared laser and terahertz Process Tomography (PT) [18,19]. Ozanyan et al. also performed research involving terahertz PT [20]. A group from Guangdong University of Technology, China, studied the fan beam optical sensor approach and its application in mass flow rate measurement of pneumatically conveyed solids [21,22]. At the Beijing Institute of Petrochemical Technology, Yan et al. implemented optical tomography using optical fiber with the addition of artificial intelligent elements in their design [23].

2.2. The selection of the optical sensor and projection arrangement

The selection of optical sensors is crucial in designing an optical tomography system. To ensure that the system will operate efficiently, a comprehensive selection of the sensors must be performed. The selection of the sensors is influenced by the projection arrangement of the chosen optical sensors, i.e., parallel beam mode or fan beam mode.

For parallel beam mode, the sensors detect light from a narrow angle beam, while the fan beam mode uses a source emitting a wide angle beam. Both types of projections, the parallel- and fan-beam modes, have their own advantages and disadvantages. The main difference between the parallel beam and fan beam modes is depicted in Fig. 1.

In the parallel beam projection mode, the sensors are arranged such that one transmitter corresponds to one receiver. In the fan beam projection mode, one transmitter is used with several receivers. As shown in Fig. 1(a), parallel beam projection is simple

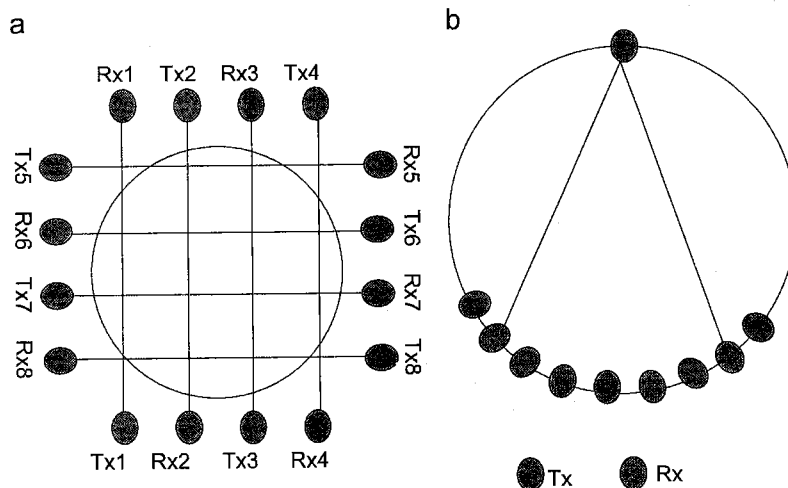


Fig. 1. (a) Parallel beam projection and (b) fan beam projection.

and easy to implement because all the transmitters and receivers will be 'ON' at the same time, and no switching control is required for the transmitter. However, this simple construction exhibits poor coverage because the light beam path is straight, so only certain parts of the sample will be measured. Blank spots or parts that cannot be detected will adversely affect the tomogram result.

In the fan beam projection mode, as shown in Fig. 1(b), 100% of the pipe cross-section is covered. However, the vital drawback of this mode is that the switching process of the detectors from one transmitter to the next, until the entire transmitter array is finished performing the scanning, critically lengthens the detection period. Investigations were performed to identify the best detection for optical tomography by coupling the different sensor methods to different beam modes. The investigated groups are listed below:

- (a) Fiber optic and parallel beam mode [9,10].
- (b) LED and fan beam mode [24,25].
- (c) Infrared and parallel beam mode [12,13,26].
- (d) Infrared and fan beam mode [27].
- (e) Laser and parallel beam mode [14].
- (f) Laser and fan beam mode [18].
- (g) Dual mode [11,17,28].

According to previous researchers [11,18,27], the fan beam technique offers better performance in comparison to the parallel beam approach. The parallel beam approach provides a limited number of measurements, thus lowering the resolution. To improve the performance of parallel beam projection, Muji et al. developed a combination of the fan beam and parallel beam approaches. This configuration demonstrated improved resolution [29]. However, the speed of the measurement was lower, due to the large number of measurements required. Therefore, the solution is to choose a sensor that has a fast response. In terms of sensor selection, the majority of the researchers used an optoelectronic device in their work because it is easier to handle than the fiber optic sensors. A laser diode is preferred because of its collimation factor and narrower beam of light. Meanwhile, an infrared laser is chosen because of the eye safety features relative to that of optical lasers. Pang [12], Goh [13] and Chiam [26] indicated that there were three factors that can influence the collimation of light: (1) the sensor to be used must have a small view angle; (2) no divergence of light between adjacent sensors should occur, i.e., an aperture must be located in front of the sensors; (3) alternate arrangements between transmitters and receivers can avoid light from one transmitter overlapping with another. In this paper, this problem of overlapping transmitters is solved by using a switching technique in the transmitter section. The switching technique prevents the receiver from receiving an incorrect signal from an adjacent emitter. The selection of the sensors must meet certain criteria: all of the incident light on the surface of an object is fully absorbed by the object, and the effects of light scattering and beam divergence are neglected [30]. Other criteria, such as low cost, small physical size, luminous intensity, high setting time, high transient characteristics, projection angle and wavelength must also be taken into consideration [31].

The hardware design in this study is discussed in the following section. The novelty of the hardware design is in the unique combination between the fan beam and parallel beam projection modes, which is proven to provide a uniform representation of the image. The improvement in the previous design is in terms of a better NMSE value for the full flow model, which is valid when the pipe is being tested with an object that fills the overall diameter. When compared with the work of Goh, 2005 [13], the NMSE for our system is 0.005, while Goh only achieved a value of 0.66. For the half-flow model, our system also showed improvement because it achieves a value of NMSE of 0.51, while Goh only achieved a value of approximately 4.6. This improvement is due to

the combination strategy, called MPFB, that was implemented, which is a mix of projections of the parallel and fan beam projections. The strategy uses a switching technique to perform the mixed projection. The combination technique is shown in Fig. 2, which gives an overview of the fan beam projection, parallel beam projection and the combination of both projections.

3. Hardware development

The majority of the previous research studies implemented the fan beam projection mode rather than parallel beam projection mode [32]. This preference for the fan beam mode is due to the advantages of the fan beam mode over the parallel beam mode; although the fan beam mode requires time to implement the switching process, it can cover a greater range. Moreover, by using a switching mode, the hardware system can handle a large current, which can prolong the lifetime of the system. Parallel beam projection requires a much shorter data acquisition time because all the sensors simultaneously acquire data. However, the parallel beam projection mode cannot cover the entire range because the straight lines of light only cover certain locations in the pipe. To address this reduced coverage problem of the parallel beam mode, a combination of parallel and fan beams is proposed. This combination of modes uses a switching/pulsing technique because the technique allows groups of emitters and photosensors to operate independently [33].

The optical tomography system consists of three important sub-systems, namely a sensor array, a signal conditioning unit and a data acquisition unit. Fig. 3 shows the overall configuration for an optical tomography system for solid gas measurement. As shown in Fig. 3, a master unit will control the slave unit to provide a signal to the light projection circuit. The receiver will respond to the light detected, and after processing the three steps of providing current to the voltage converter, amplifying the signal and sending the signal through the voltage divider, the voltage value will loop back to the slave unit. In this step, the slave unit will convert the analog signal to a digital signal. This digital signal will be stored in the slave's buffer until the user clicks on the GUI in the PC to activate the master unit to enable the collection of all the data using the I2C protocol. Once the data have been accepted by the master, the data will be transmitted to the PC via the RS232 protocol.

3.1. Sensor selection

Before designing the sensor circuit, the selection of the sensors to use must be made. Many factors should be taken into consideration when choosing a pair of sensors in optical tomography, such as a spectral range that matches the emission wavelength of the emitter [33], the appropriate half angle between them and the rise- and fall-time. For the receiver circuit, the projection style will influence the timing. The switching method requires a longer data acquisition time relative to having the sensors being "on" simultaneously. Therefore, for the switching technique, a photodiode is superior to a phototransistor, as a fast response speed is critical in a switching system [33].

3.1.1. Photodiode selection

After a number of observations and research, a SFH229FA photodiode was selected. The important characteristics for this sensor are as follows:

- i) Spectral range of sensitivity between 730 nm and 1100 nm. This range is for response in the infrared range and was selected because visible light is outside this range, thereby

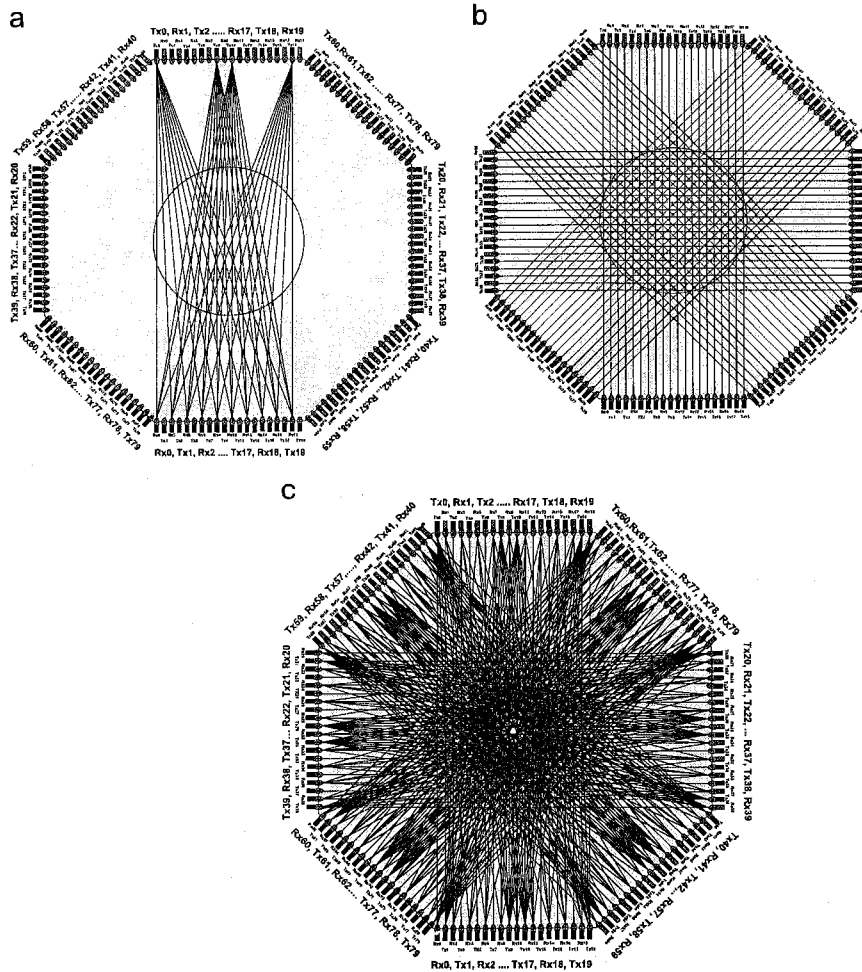


Fig. 2. (a) Fan beam projection, (b) parallel beam projection and (c) MPFB.

reducing the noise. The SFH229FA photo-detector has a spectral range of sensitivity in the infrared, with a peak wavelength of 900 nm. A transmitter was selected to emit in this infrared spectral range.

- ii) Fast switching time of 10 ns.
A fast switching time is needed to minimize the data acquisition time of this system. Moreover, the concept used in this system is a combination of the parallel- and fan-beam projection modes, where rapid time switching is crucial to ensure that the system can produce an image.
- iii) Half angle of $\pm 17^\circ$.
This angle was selected because it is acceptable for use in both the parallel beam mode and the fan beam mode. For the parallel beam mode, any value is not a problem because switching of the transmitter source is used, while for the fan beam mode, $\pm 17^\circ$ of half angles is considered to be sufficient to receive the signal.

3.1.2. Transmitter sensor selection

In this project, an infrared emitting diode, TSUS 4300, was used as the transmitter. TSUS 4300 is a Gallium Arsenide (GaAs) [34] type of infrared emitter. The GaAs type of emitter emits infrared energy efficiently and is the primary selection for use in optical

switches [33]. The TSUS emitter exhibits matching characteristics with regards to the selected photodiode. Some of the factors involved in this selection are as follows:

- i) Spectral range of emission between 915 nm and 990 nm.
The range matches the receiver and the peak wavelength is 950 nm, which is close to the receiver's peak wavelength of 900 nm.
- ii) Switching time.
Both the fall- and rise-time is 800 ns. This value is greater than the switching time for the receiver, which is only 10 ns, but it is acceptable.
- iii) Half angle of $\pm 16^\circ$.
The half angle is almost the same as that of the receiver, and it is in the range of the receiver coverage. Therefore, it is a suitable transmitter for the selected receiver.

3.2. Optical circuit

For the transmitter circuit, the criteria of fast switching and the ability to transmit a signal are important; for the receiver circuit, a fast response and a high sensitivity are required. The sub-sections below will discuss this further.

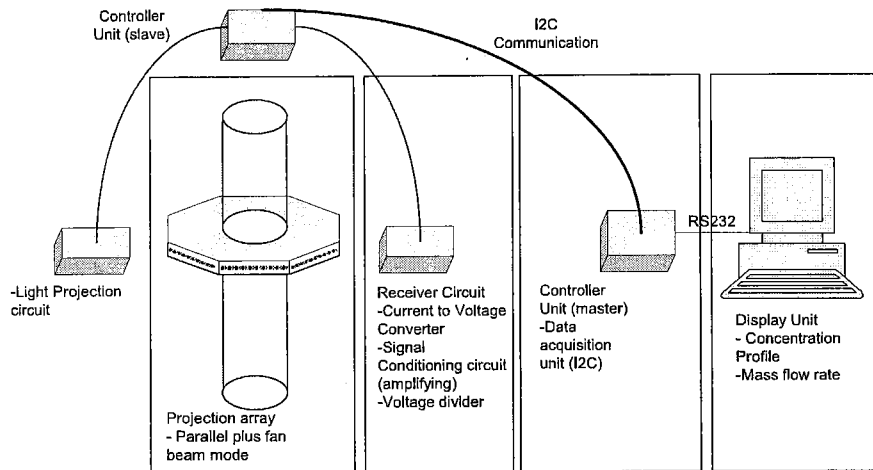


Fig. 3. Optical tomography system.

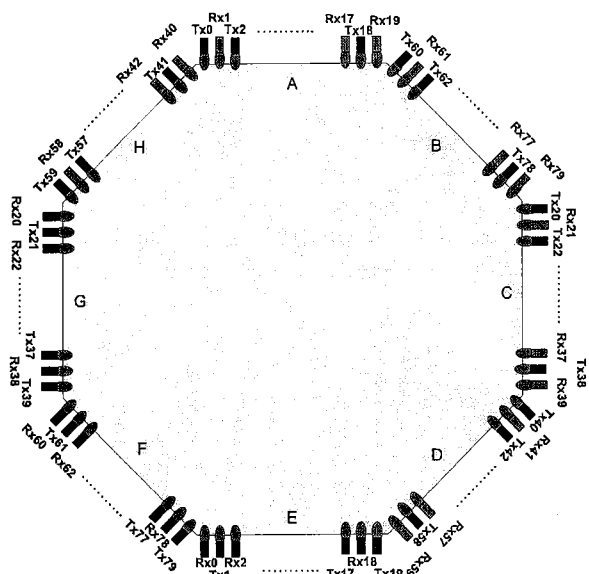


Fig. 4. Sensor numbering in the optical tomography setup.

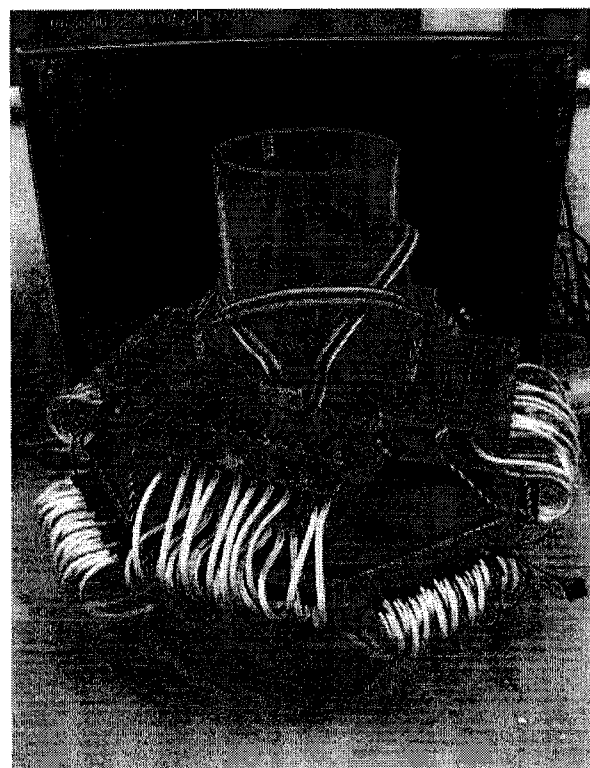


Fig. 5. Overall system.

Table 1 Receiver numbering and corresponding location for saving the data from sides A and E.

Side A		Side E	
Buffer	Receiver	Buffer	Receiver
Store [0]	Rx0	Store [1]	Rx1
Store [2]	Rx2	Store [3]	Rx3
Store [4]	Rx4	Store [5]	Rx5
Store [6]	Rx6	Store [7]	Rx7
Store [8]	Rx8	Store [9]	Rx9
Store [10]	Rx10	Store [11]	Rx11
Store [12]	Rx12	Store [13]	Rx13
Store [14]	Rx14	Store [15]	Rx15
Store [16]	Rx16	Store [17]	Rx17
Store [18]	Rx18	Store [19]	Rx19

Table 2 Speed for different types of projection.

Type of projection	Speed (frame/second)
Parallel beam	62
Fan beam	26
MPPB	12

The technique used to transfer the data from the receiver side to the monitor is through sending the data back to the microcontroller (slave). In this way, both the transmitter and receiver can be effectively

synchronized. The data will be converted into digital form and will then be sent to another microcontroller (master). The master unit will then arrange for the activation of every microcontroller (slave).

For transferring the data to the PC, the RS232 protocol is used to acquire the data that has been collected in the master memory. RS232 is able to send data to a computer at a variety of speeds, and 115200 bps was used in this research. Here, the synchronization between the microcontroller (hardware) and the Visual Basic (VB) program is very important. In the hardware section, the master microcontroller collects all the data from the slave. The numbering of the sensors is set to define the correct arrangement. Fig. 4 shows the numbering of the sensors used in this research, where every side has its own slave microcontroller to collect the analog data from the receivers.

The setup has eight sides, named A, B, C, D, E, F, G and H. Slave A will collect data from the receivers on side E, whose detectors are interacting with the transmitters controlled by slave A. The collected data are stored in the buffer in sequence; for example, for slave A, the data that follows the numbering of sensors, listed in Table 1, is saved. Slave E will store the data from the receivers on side A.

Fig. 5 shows an image of the complete hardware system.

4. Results and discussion

In this paper, optical tomography measurements are performed to evaluate the concentration profile, NMSE and PSNR. Because this system is a mixed projection of fan beams and parallel beams the measurement is performed in sequence, where the parallel beam is first activated by a microcontroller, followed by the fan beam being activated. The parallel beam projection scheme involves 80 measurements (sensor pairs) and the fan beam

projection scheme involves 320 measurements, i.e., a total of 400 measurements are required for the mixed projection system. Therefore, 400 measurements are acquired for one frame of data. Table 2 lists the speed of capturing one frame of data for the parallel beam, fan beam and MPFB projection modes.

4.1. Concentration profile (%)

An experiment was performed using the flow rig shown in Fig. 6(a). The optical tomography system was located at the bottom of the pipe to ease the process of installing the system in a gravity flow rig, as shown in Fig. 6(b). Based on the observations, the resolution that can be achieved by this system is 64×64 pixels. The pipe used for the experiments was 100 mm in diameter, and the loading rate used can be up to a maximum of 900 g/s. An image of the complete optical tomography system is shown in Fig. 6(c).

Plastics beads were used in the mass flow rate experiment because they can be recycled numerous times. The bead average diameter is 2.7 mm and the bead height is 3.3 mm. The purpose of this experiment was to determine whether the sensor is able to respond to the flow pattern inside the pipe using three different sizes of baffles (shown in Fig. 7).

Each of the projection modes was tested to determine the performance of each in characterizing a real flowing system.

The sensor system was placed at different locations to determine the best sensor location for detecting an accurate flow. The three different locations used are illustrated in Fig. 8.

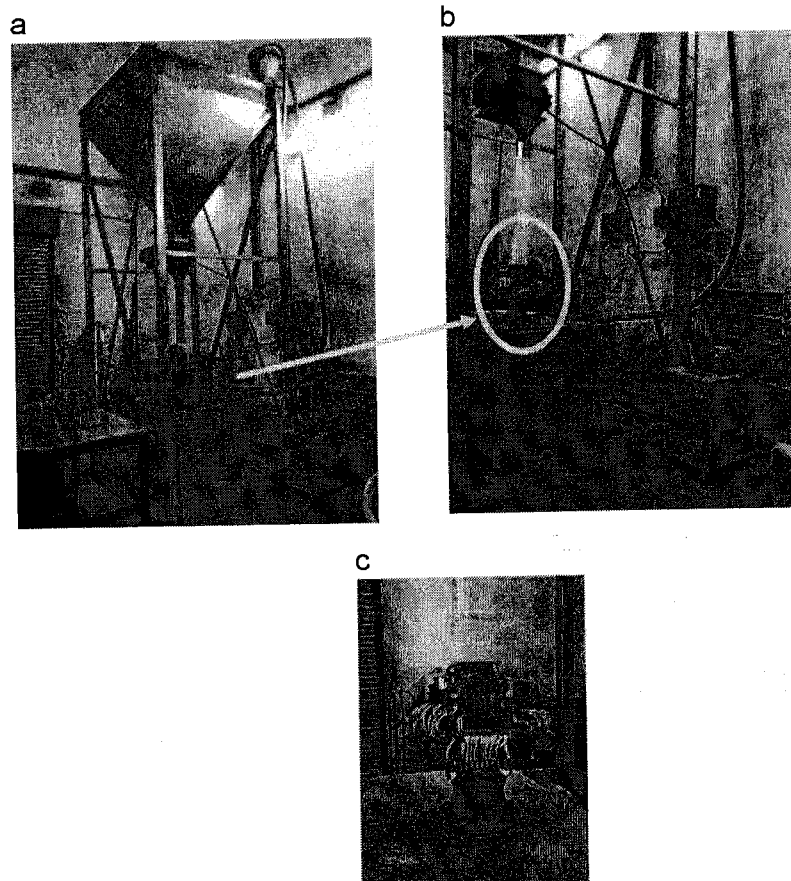


Fig. 6. Gravity flow rig: (a) actual flow rig, (b) after installation of the optical tomography system and (c) the optical tomography system.

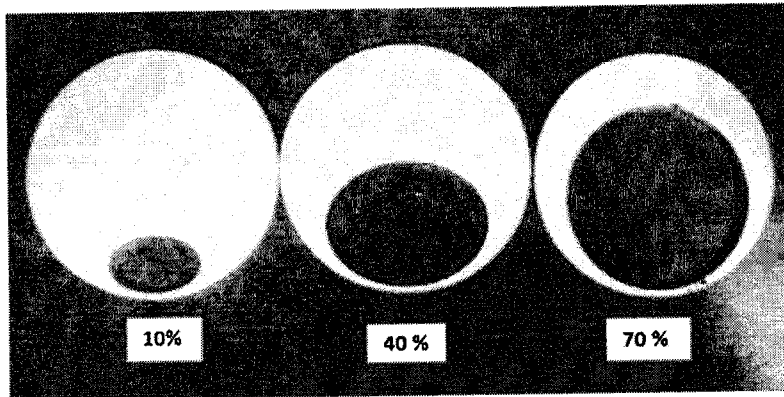


Fig. 7. Three different baffle sizes.

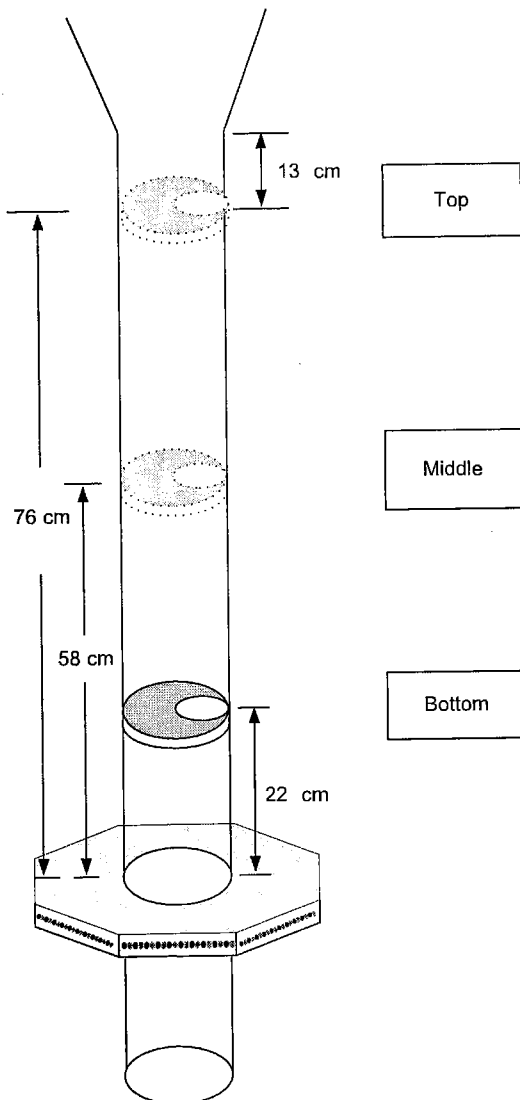


Fig. 8. Three different locations of the baffle placement.

To conduct the concentration profile measurements, 3 types of baffles were used to determine whether the material flow in the pipe follows the shape of the baffle. As mentioned by Yan, the sensing techniques for the concentration measurement of solids are classified into four main groups: electrical, attenuation, resonance and tomography [35]. This experiment examined the concentration distribution using the tomography method.

To acquire the concentration profile, the calibration was performed by setting a zero flow in the experimental pipe and measuring the voltage of each receiver for each transmitter projection, followed by storing the measured voltage in the PC. These calibration data were required during the image reconstruction process for extracting the sensor loss information. To extract the sensor loss information from the optical receiver, the following equation was used:

$$S_L = V_{Ref} - V_M \tag{1}$$

S_L is the Amplitude of the signal loss for the projection of Tx-th to Rx-th, V_{REF} the Reference voltage for the projection of Tx-th to Rx-th and V_M Sensor value for the projection of Tx-th to Rx-th

In this paper, the Linear Back Projection (LBP) algorithm was used to reconstruct the image. In the LBP algorithm, the concentration profile is generated by integrating each sensor reading with its computed sensitivity maps [36]. The modeled sensitivity matrices are used to illustrate the image plane for each view. To reconstruct the image, each sensitivity matrix is multiplied by its corresponding sensor loss value. Next, the new values following multiplication are located into new matrices. The same elements in these matrices are summed to provide the back projected voltage distributions (concentration profile), or $V(x, y)$.

The concentration profile provides the percentage of the material inside the pipeline, and for solid gas study it provides two values: the gas concentration percentage and the solid concentration percentage. The solid and gas distributions in the tomogram are calculated using the following equations [37].

$$A_s = \frac{\sum_{y=1}^{64} \sum_{x=1}^{64} V(x, y)}{M_p} \times 100\% \tag{2}$$

$$A_G = \frac{1 - \sum_{y=1}^{64} \sum_{x=1}^{64} V(x, y)}{M_p} \times 100\% \tag{3}$$

where, A_s is the solid area percentage, A_G the gas area percentage, $V(x, y)$ the obtained pixel values for a 64×64 pixel concentration profile and M_p the total pixel value, which is 1690388.

As shown in Eq. (2), the solid area percentage is acquired by summing each of the pixel values that contribute to the concentration profile matrix and dividing by the total pixel value. A 64×64 square matrix has 4096 pixels, but only 3308 pixels are used to represent the image plane of the pipe cross-section, and a further 788 pixels lie outside of the pipe boundary. The maximum value of each pixel is 511, and therefore the total value of the pixels was calculated by multiplying 3308 pixels by 511, which resulted in a value of 1690388. The gas area percentage was obtained by simply deducting the normalized solid area from one, as shown in Eq. (3).

4.2. Baffle at the bottom

The baffle was located at the bottom of the flow pipe because the purpose of this experiment was to determine whether the blockage area in the pipe can affect the tomogram results. The baffle can also contribute to information on the sensor's performance regarding its response to the correct flow. Table 3 shows the concentration results for different flow patterns when the baffle was located in the bottom part of the flow rig. Three types of projection modes were tested: the parallel beam (PB), fan beam

(FB) and mixed projection of parallel- and fan-beams (MPFB) techniques. The results indicate that the MPFB technique produced a uniform image in which the pixels were well distributed in the tomogram. For the FB and PB techniques the image was not uniform, as there was a part that had high pixels and low pixels in the concentration image and they were not as uniform as the pixels of the MPFB projection.

4.3. Baffle at the center and at the top (MPFB)

Tables 4 and 5 show the results of using MPFB for flow patterns of 10%, 40% and 70%. The baffle was located at the center and at the top of the pipe flow rig in the two experiments, and from the data in both tables, only the 10% opening baffle exhibited the correct pattern, whereas the others were incorrect. The incorrect patterns occurred because the distance between the baffle and the sensor location is quite far and does not enable the sensor to capture the correct pattern of flow. However, the 10% baffle opening was able to produce the correct pattern because the 10% baffle produces a high pressure in the flow allowing the pattern to persist until the flow arrives at the sensor location, as shown in Fig. 9 (a). For the

Table 3
Comparison between the parallel beam, fan beam and mixed projection modes.

GAS		SOLID	
0		511	
10% Opening			
PB	FB	MPFB	
%C = 24	%C = 20	%C = 27	
40% Opening			
%C = 67	%C = 71	%C = 74	
70% Opening			
%C = 81	%C = 88	%C = 83	

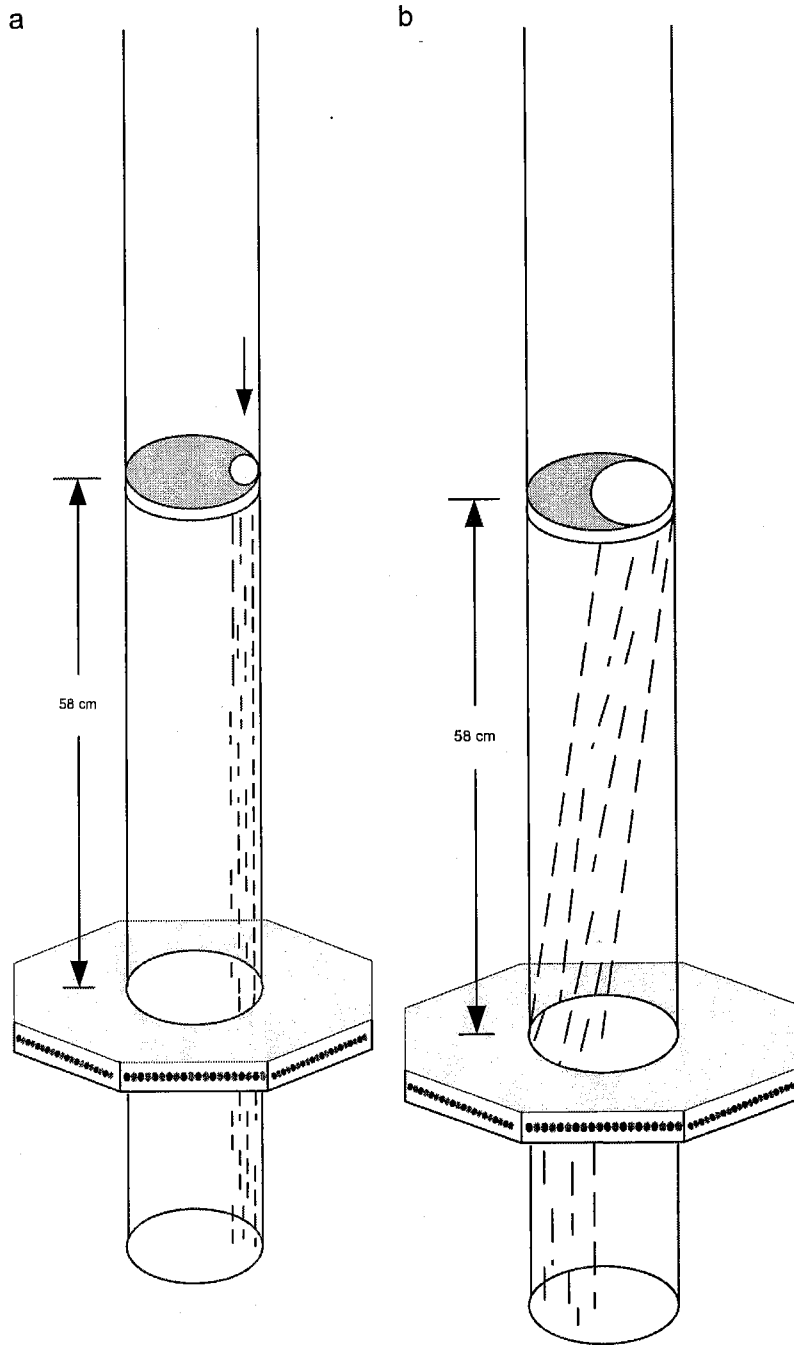


Fig. 9. Flow effect at the sensor location: (a) 10% baffle opening and (b) 40% and 70% baffle openings.

40% and 70% baffle openings, the pressure at the top is not very high because the opening is larger, and therefore the pressure is not as high as with the 10% opening. This reduced pressure resulted in the plastic beads exhibiting a low pressure while flowing through the baffle and resulted in the flows shown in Fig. 9(b).

4.4. PSNR and NMSE

Static experiments were also conducted to determine the quality of the images. For the purpose of evaluating image quality,

two important parameters were used: NMSE and PSNR. A low NMSE value and a high PSNR correspond to a high quality image. Eq. (4) is the formula used to determine the value of NMSE.

$$NMSE = \frac{\sum_{x=0}^{n-1} \sum_{y=0}^{n-1} [f(x,y) - f'(x,y)]^2}{\sum_{x=0}^{n-1} \sum_{y=0}^{n-1} f(x,y)^2} \quad (4)$$

where, $f(x, y)$ is the original image, $f'(x, y)$ is the reconstructed image and n is the number of pixels.

Table 4
Baffle at the center (MPFB).

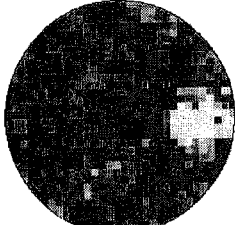
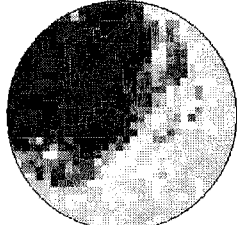
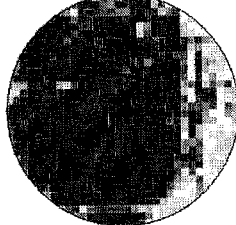
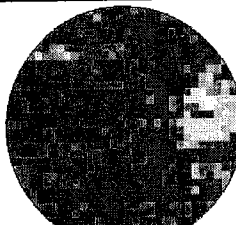
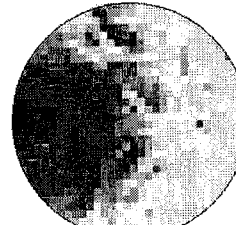
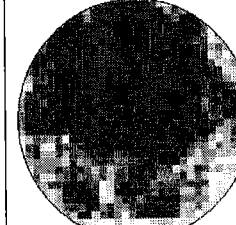
10% Opening	40% Opening	70% Opening
		
%C = 21	%C = 76	%C = 83

Table 5
Baffle at the top (MPFB).

10% Opening	40% Opening	70% Opening
		
%C = 22	%C = 75	%C = 83

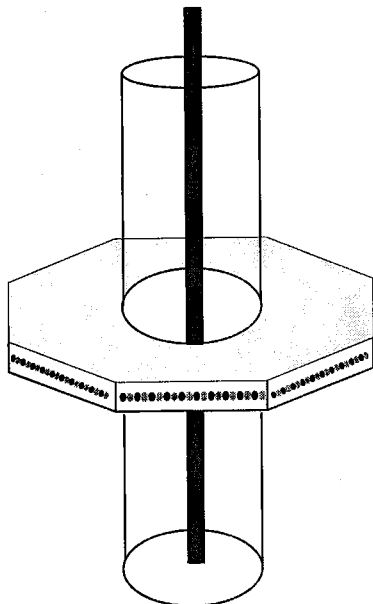


Fig. 10. Static experiment for a single object.

being identical to the original image. Eq. (5) shows the method of calculating the PSNR value.

$$PSNR = 20 \log \frac{MAX}{RMSE} \quad (5)$$

MAX is Maximum possible pixel value, RMSE=Root Mean Square Error

Here, MAX is the maximum possible pixel value of the image. In this research, the maximum possible value that has been used for every pixel is 511; therefore, the MAX value here is 511.

Fig. 10 shows the static experiment used to evaluate the improvement in the image after conducting the mixed projection technique. Initially, the projection was programmed to act as parallel beam projection. After the image was captured, the setting was changed to fan beam projection mode. Finally, the projection setting was changed to the combination of the parallel- and fan-beam projections.

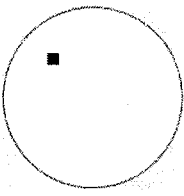
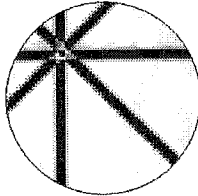
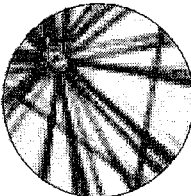
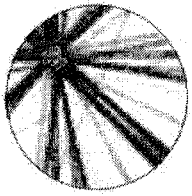
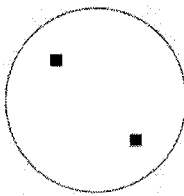
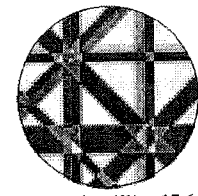
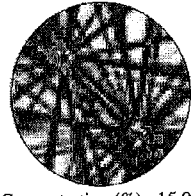
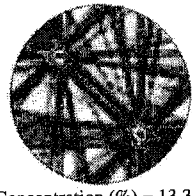
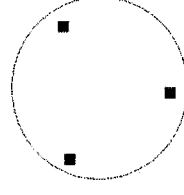
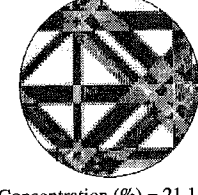
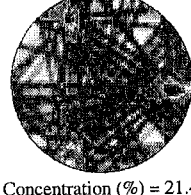
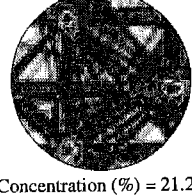
The results demonstrate a significant improvement when the MPFB technique was used. Table 6 shows the results for the static experiments for three different object locations in the pipe. The results demonstrate that with the combination of the parallel- and fan-beam projection techniques, the values of PSNR are significantly increased. In addition, the NMSE value exhibits a decreasing trend when the MPFB mode is used.

5. Conclusion

In conclusion, the results of this research demonstrate several improvements and achievements. The ability to implement fan

The PSNR value is dependent on the MSE value: if the MSE approaches a value of zero, then the PSNR will approach infinity, which corresponds to the situation of the reconstructed image

Table 6
Comparison between single projection modes and the combined projections.

Object	Parallel beam (PB)	Fan Beam(FB)	Combination of parallel and fan beams (MPFB)
	 Concentration (%) = 5.7 PSNR (dB) = 19.7 NMSE = 3.7	 Concentration (%) = 8.0 PSNR (dB) = 19.7 NMSE = 3.7	 Concentration (%) = 6.4 PSNR (dB) = 21.1 NMSE = 2.6
	 Concentration (%) = 17.6 PSNR (dB) = 13.7 NMSE = 6.3	 Concentration (%) = 15.9 PSNR (dB) = 15.2 NMSE = 4.5	 Concentration (%) = 13.3 PSNR (dB) = 16.7 NMSE = 3.1
	 Concentration (%) = 21.1 PSNR (dB) = 12.5 NMSE = 4.8	 Concentration (%) = 21.4 PSNR (dB) = 13.0 NMSE = 4.3	 Concentration (%) = 21.2 PSNR (dB) = 13.3 NMSE = 4.0

beam projection in parallel view is one of the novelties of this research. The sensor jig is specifically designed for parallel applications that do not involve a collimator design. Therefore, fan beam projections can also be implemented in the same sensor jig without difficulty. The method utilized to overcome the disadvantages of parallel beam projection is a practical solution to the problems that arise with a parallel beam. Significant progress was achieved when the combination of the parallel- and fan-beam methods was successfully developed, as it produces a uniform image in which the entire pixel is well distributed in the tomogram. The combination method also produced better PSNR and NMSE values, which illustrates that it produces high quality images. The system using the combination of parallel- and fan-beam modes also responds well when a baffle is located at the bottom of the pipe, and the results demonstrate that the system can detect any blockage that is near the optical tomography system.

References

[1] Ai M. Future of imaging technology. *Sensors and Actuators A: Physical* 1996;56 (1–2):31–8.

[2] York T, McCann H, Ozanyan KB. Agile sensing systems for tomography. *IEEE Sensors Journal* 2011;11(12):3086–104.

[3] Plaskowski A, Beck MS, Thorn R, Dyakowski T. *Imaging industrial flows*. London: Institute of Physics Publishing Ltd.; 1995.

[4] Industrial Visit Report: Sime Darby Pulau Carey Banting; 2011.

[5] Global Spec. Solids flow meters. Available from: (http://www.globalspec.com/learnmore/sensors_transducers_detectors/flow_sensing/flomimeters_solids) [Retrieved 29.11.11].

[6] Dickin FJ, Hoyle BS, Hunt A, Huang SM, Ilyas O, Lenn C, Waterfall RC, Williams RA, Xie CG, Beck MS. Tomographic imaging of industrial process equipment: techniques and applications. *IEEE Proceeding on Circuits, Devices and Systems* 1992;139(1):72–82.

[7] Jing L, Liu S, Zhihong L, Meng S. An image reconstruction algorithm based on the extended Tikhonov regularization method for electrical capacitance tomography. *Measurement* 2009;42(3):368–76.

[8] Dugdale P, Green RG, Hartley AJ, Jackson RG, Landauro J. *Optical sensors for process tomography*. ECAPT Manchester 1992:26–9.

[9] Abdul Rahim R. A tomography imaging system for pneumatic conveyors using optical fibres. Sheffield Hallam University; 1996 Doctor Philosophy.

[10] Ibrahim S. Measurement of gas bubbles in a vertical water column using optical tomography. Sheffield Hallam University; 2000 Doctor Philosophy.

[11] Chan KS. Real time image reconstruction for fan beam optical tomography system. Universiti Teknologi Malaysia; 2002 Master Engineering.

[12] Pang JF. Real-time velocity and mass flow rate measurement using optical tomography. Skudai: Universiti Teknologi Malaysia; 2004 Master Engineering.

[13] Goh CL. Real-time solids mass flow rate measurement via ethernet based optical tomography system. Universiti Teknologi Malaysia; 2005 Master Engineering.

[14] Mohamad EJ. Flame imaging using laser based transmission tomography. Universiti Teknologi Malaysia; 2005 Master Engineering.

- [15] Abdul Rahim R, Leong LC, Chan KS, Rahiman MH, Pang JF. Real time mass flow rate measurement using multiple fan beam optical tomography. *ISA Transaction* 2008;47(1):3–14.
- [16] Abdul Rahim R, Chiam KT, Puspanathan J, Susiapan YS-L. Embedded system based optical tomography: the concentration profile. *Sensor Review* 2009;29(1):54–62.
- [17] Rasif MZ. The development of a Dual Modality Tomography (DMT) system using optical and capacitance sensors for solid/gas flow measurement. *Universiti Teknologi Malaysia*; 2009 Master Engineering.
- [18] Chen J, Hou D, Zhang T, Zhou Z. Near infrared laser computed tomography test-system design and application. *Flow Measurement and Instrumentation* 2005;16(5):321–5.
- [19] Zhang G-X, Chen J, Zhou Z-K. Terahertz PT technology for measurement of multiphase flow and its infrared simulation. *Journal of Zhejiang University Science* 2005;6A(12):1435–40.
- [20] Ozanyan KB, Wright P, Stringer MR, Miles RE. Hard-field THz tomography. *IEEE Sensors Journal* 2011;11(10):2507–13.
- [21] Li Y, Zheng Y-N, Yue H-W. Design of fan beam optical sensor and its application in mass flow rate measurement of pneumatically conveyed solids. *Zhejiang University Science A* 2005;6A(12):1430–4.
- [22] Zheng Y, Liu Q, Li Y, Gindy N. Investigation on concentration distribution and mass flow rate measurement for gravity chute conveyor by optical tomography system. *Measurement* 2006;39(7):643–54.
- [23] Yan C, Zhong J, Liao Y, Lai S, Zhang M, Gao D. Design of an applied optical fiber process tomography system. *Sensors and Actuators B: Chemical* 2005;104(2):324–31.
- [24] Zeng N, Lai S, Liao Y. Optical tomography for two phase flow measurement. *Proceedings of SPIE—The International Society for Optical Engineering* 2001;4448:341–7.
- [25] Chen A, Yang Y, Alqasemi U, Aguirre A, Zhu Q. A low cost multi-wavelength tomography system based on LED sources. *Progress in Biomedical Optics and Imaging—Proceedings of SPIE* 2011:7896.
- [26] Chiam KT. Embedded system based solid-gas mass flow rate meter using optical tomography. *Universiti Teknologi Malaysia*. 2006 Master Engineering.
- [27] Leong LC. Implementation of multiple fan beam projection technique in optical fibre process tomography. *Universiti Teknologi Malaysia*. 2005 Master Engineering.
- [28] Rzasa MR. The measuring method for tests of horizontal two-phase gas-liquid flows, using optical and capacitance tomography. *Nuclear Engineering and Design* 2009;239(4):699–707.
- [29] Muji SZM, Abdul Rahim R, Rahiman MH. Sensitivity Map in Parallel and Fan Beam mode in Optical Tomography. In: *Proceedings of the 6th World Congress on Industrial Process Tomography (WC IPT6)*: Beijing, China; 2010 pp. 762–771.
- [30] Abdul Rahim R, Pang JF, Chan KS. Optical tomography sensor configuration using two orthogonal and two rectilinear projection arrays. *Flow Measurement and Instrumentation* 2005;16(5):327–40.
- [31] Abdul Rahim R, Chan KS, Pang JF, Leong LC. A hardware development for optical tomography system using switch mode fan beam projection. *Sensors and Actuators A: Physical* 2005;120(1):277–90.
- [32] Muji SZM, Abdul Rahim R, Rahiman MHF, Abdul Shaib MF, Sahlan S, Jaysuman Muhammad, et al. Optical tomography: a review on sensor array, projection arrangement and image reconstruction algorithm. *International Journal of Innovative Computing, Information and Control* 2011;7(7A):3839–56.
- [33] Birtalan D, Nunley W. *The photodiode infrared-visible-ultraviolet devices and applications*. 2nd Ed. Boca Raton F.L.: CRC Press; 2009.
- [34] Vishay semiconductor. TSUS4300 Infrared Emitting Diode, 950 nm, GaAs. Available from: (<http://www.vishay.com/docs/81053/tsus4300.pdf>); 2005 [Retrieved 13.12.09].
- [35] Yan Y. Mass flow measurement of bulk solids in pneumatic pipelines. *Measurement Science and Technology* 1996;7:1687–706.
- [36] Green RG, Rahmat MF, Evans K, Goude A, Henry M, Stone JAR. Concentration profiles of dry powders in a gravity conveyor using an electrodynamic tomography system. *Measurement Science and Technology* 1997;8:192–7.
- [37] Rahiman MHF, Rahim RA, Rahiman MHF, Tajjudin M. Ultrasonic Transmission-Mode Tomography Imaging for Liquid/Gas Two-Phase Flow. *Sensors Journal, IEEE* 2006;6(6):1706–15.